Solid Freeform Fabrication 2019: Proceedings of the 30th Annual International
Solid Freeform Fabrication Symposium – An Additive Manufacturing Conference
Reviewed Paper

PREDICTING AND CONTROLLING THE THERMAL PART HISTORY IN POWDER BED FUSION USING NEURAL NETWORKS

Holger Merschroth[1], Michael Kniepkamp[1], Matthias Weigold[1]

[1] Institute of Production Management, Technology and Machine Tools (PTW),
Technische Universität Darmstadt, Darmstadt, Germany

Abstract

Laser-based powder bed fusion of metallic parts is used widely in different branches of industry. Although there have been many investigations to improve the process stability, thermal history is rarely taken into account. The thermal history describes the parts' thermal situation throughout the build process as a result of successive heating and cooling with each layer. This could lead to different microstructures due to different thermal boundary conditions. In this paper, a methodology based on neural networks is developed to predict and control the parts' temperature by adjusting the laser power. A thermal imaging system is used to monitor the thermal history and to generate a training data set for the neural network. The trained network is then used to predict and control the parts temperature. Finally, tensile testing is conducted to investigate the influence of the adjusted process on the mechanical properties of the parts.

1. Introduction

Additive manufacturing (AM) is an emerging field in manufacturing technologies that has the common principle of building up solid parts directly from three dimensional computer aided design (3D CAD) data by adding material layer by layer. Powder bed fusion-based processes use thermal energy to selectively fuse regions of a powder bed [1]. Powder bed fusion is a process where powder is applied in layers and then selectively melted using a laser beam to generate three-dimensional parts directly from CAD data. This study focuses on powder bed fusion of metal powder using a laser beam (PBF-LB/M). PBF-LB/M typically involves layer thicknesses between 20 and 100 µm, using powders with particle sizes ranging from 10 to 45 µm [2].

As AM is a rather new manufacturing process, important information and experience are often lacking to assess quality and part reliability. Non-destructive testing in particular allows the full benefits of AM to be utilized. Small series and single part production can be qualified and certified for destructive testing without additional identical parts [3]. The layer-wise build-up allows a three-dimensional evaluation of the part during the manufacturing process by evaluating and interpreting the process phenomena [4,5]. Monitoring systems record and interpret the physical quantities generated by process phenomena. Grasso et al. provides an overview of work already carried out [6]. Examples of process phenomena are the luminous intensity of the melt pool [7] or the vibrations caused through contact between the recoater and parts during coating [8]. The luminous intensity of the molten bath changes in areas of poor heat conduction, such as overhangs or areas disturbed by pores [9,10]. Another process phenomenon is the time-dependent part temperature. This can be determined using a thermographic camera by correlating the infrared emissions with the emission coefficient. Various boundary conditions have an influence on the part

temperature during the building process. Two main boundary conditions are the layer time and the building height [11].

In this work, the influence of thermal history on mechanical properties is investigated. Using a thermographic camera, the influence of the part height and the layer time on the temperature development is examined, as well as the influence of these factors on the mechanical properties of the components. The focus is on predicting the thermal part history using a neural network and adjusting the process parameters to reduce the influence of the thermal history on the mechanical properties. The thermal history is determined by means of a thermographic camera and the average layer temperature in every layer.

2. Research methodology

A commercially available PBF-LB/M system M290 from the EOS GmbH (Krailling, Germany) is used to conduct the experiments. This system uses a 400-W single-mode fibre laser with a wavelength of 1064 nm focused to a spot size of 83 µm. The building volume has a size of 250 mm x 250 mm x 325 mm. Gas atomized stainless steel 316L powder is used for all experiments in this study. A scanning electron microscope (SEM) analysis of the powder is used to determine the particle distribution. Particles ranging from 11 to 54 µm and a d_{50} of 25 µm was determined. The parameter set "316L_Surface_M291 1.10" with a layer thickness of 20 µm qualified by the system manufacturer is used as a reference. The PBF-LB/M system is extended by a thermographic camera to measure the parts' temperatures and the thermal history of the parts. A model of the type VarioCAM HD head 800 (InfraTec GmbH, Dresden, Germany) is used. Due to the constructional limitations of the PBF-LB/M system, the optical axis of the thermographic system is not perpendicular to the building platform, but is at an angle of approximately 19°. The distance of the camera to the construction level is approximately 530 mm. Using a 60-mm lens, an area of approximately 125 x 125 mm² around the centre of the building platform can be focused with a resolution of 0.3 mm/px. The recording rate of the camera is fixed at 30 Hz with calibration to a temperature range of 0–500 °C.

As the surface of the PBF-LB/M parts does not represent an ideal black body during the building process, the emissivity of the part surface and the powder has to be determined. According to VDI/VDE 3511 4.5 [12], the emissivity can be determined at the object to be measured under real conditions using various methods. One option is a comparison with a tactile temperature measurement on the measured object; another is to partially apply a black matt lacquer to the surface to achieve a high emissivity and to compare the temperature with the uncoated surface. In the following, both methods are carried out and the results compared with each other. The test procedure is shown in Figure 1 (top). First, a test specimen with an edge length of 30 mm and a height of 15 mm is fabricated with the basic parameter set. Then, the building platform is removed from the machine and half of the sample surface is painted with a black lacquer. After reinstalling the construction platform in the system, a type K thermocouple is applied to the untreated surface of the test specimen. In the software of the thermographic camera, a correction field with a size of 10 x 20 mm² and a definable emission coefficient is now placed on the uncoated surface of the sample. In the next step, the building platform heating is switched on and the temperatures of the thermocouple (T_t) and the average temperature of the coated surface (T_s) and the correction surface ($T_{\varepsilon b}$) are compared. The results are shown in Figure 1 (bottom).

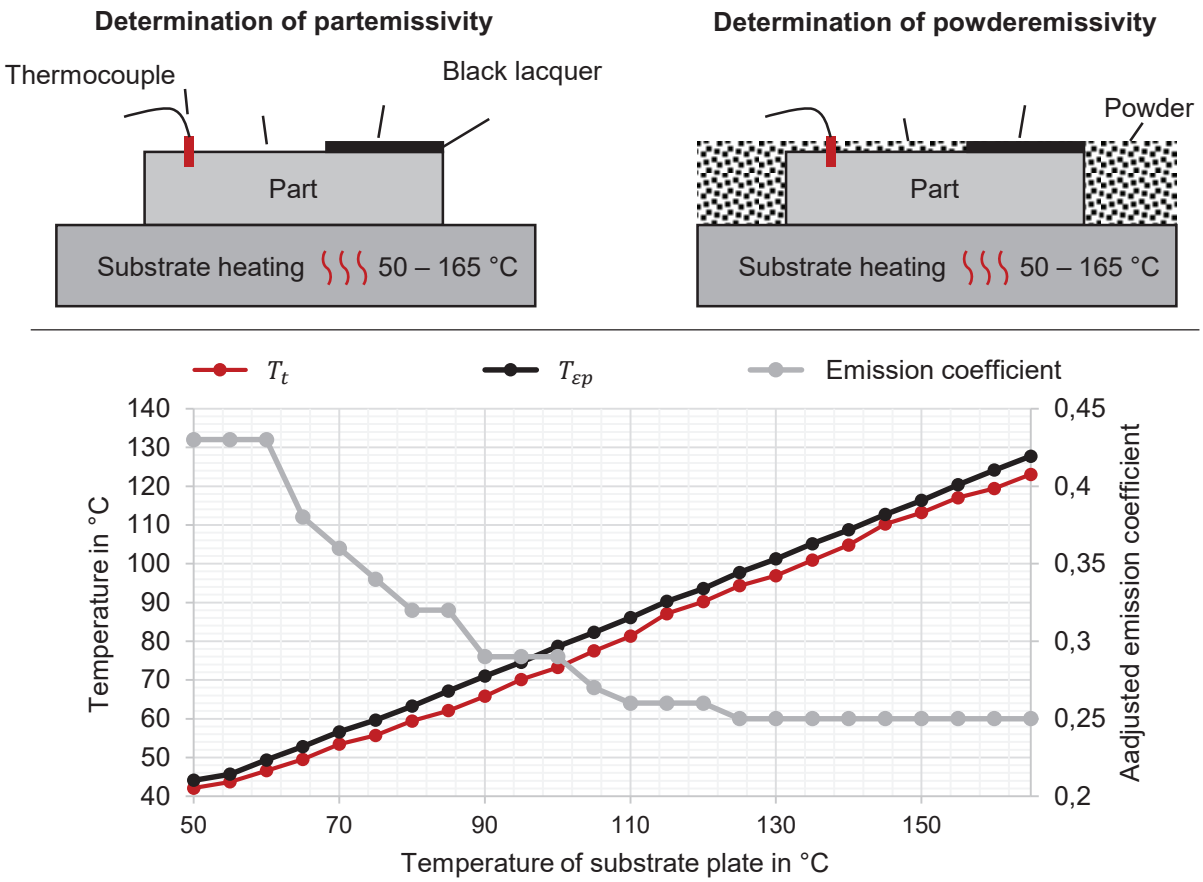

Figure 1: Schematic illustration of the emissivity determination (top) and results of the experimental determination of the emission coefficient of the powder (bottom)

Using the thermographic camera, the influence of the parameters layer time, exposure parameters and part-dependent geometric parameters on temperature development is examined, as well as whether these parameters have a direct effect on the mechanical characteristics of the parts. Three steps are carried out for this purpose. First, the influence of different parameters on the temperature development is investigated. The layer-wise averaged temperature per part during the measurement of the surface immediately before the exposure is determined as the characteristic value for the thermal history. Subsequently, different building jobs are built and the thermal development of each part is measured. The temperature prediction is then realized by a neural network that has been trained with the generated data. In the last step, the temperature is homogenized by adjusting the process parameters. Using the neural network, the process parameters are then adjusted layer by layer so that a critical temperature is not exceeded. The influence of the thermal history on the mechanical properties is determined by tensile testing. For this purpose, cylindrical specimens for tensile tests with a diameter of 10 mm and a height of 83 mm are manufactured.

The layer time, that is, the time between two successive exposure steps, is varied in three steps. The minimum layer time (t_{s_min}) for the combination of machine and basic parameter set used is 16.68 s for four tensile specimens on the building platform. The second layer time (t_{s_20}) simulates a surface utilization of about 20% of the building platform area and amounts to 25 s. The third layer time (t_{s_∞}) represents the quasi-static case, in which after each exposure process, the

system waits until no further temperature change is detected. To avoid a mutual influence of the samples, they are placed at a distance of 50 mm from each other on the building platform. For the layer times t_{s_20} and t_{s_∞}, six samples are prepared in one building job; for the layer time t_{s_min}, two building jobs with four samples each are built. During the building process, an exposure step is recorded with the thermographic camera every 25 layers. For each sample, the part temperature averaged over the complete cross-section of the sample is recorded at a rate of 30 Hz. The temporal temperature curve of such a measurement is shown in Figure 2. The measurement can be divided into four areas. In the first section, the part is coated with new powder. An apparent drop in temperature can be observed here, which is caused by the recoater covering the sample. The second section follows, in which the part surface is covered with a layer of powder. The characteristic feature is an apparent increase in temperature compared with the cooling phase. The actual exposure of the part takes place in the third section. A temperature measurement in this range is not possible with the test set-up because the recording rate is too low, the temperature exceeds the calibrated range of 0-500 °C and the emissivity of the molten bath is unknown. The fourth area represents the cooling phase in which the remaining parts are exposed, the building platform is moved to the next part height and the coater returns to the exit position. To determine the part temperature over the entire construction process, the average temperature at the time shortly before exposure is selected for each measurement (t_{mess}). Since the part cross-section is covered with powder at this time, the emission coefficient (ε_p) of the powder of 0.45 is used.

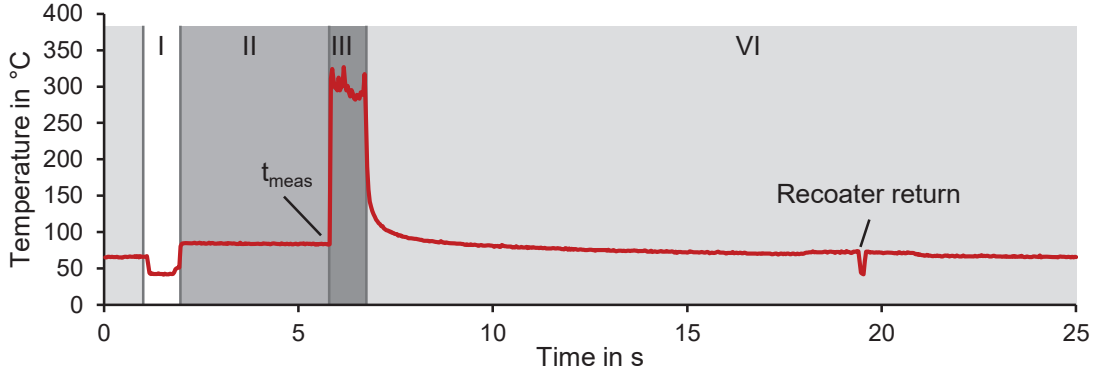

Figure 2: Temperature curve of the part surface during one layer cycle

In addition to the layer time, the area energy input by the laser represents a geometry-independent factor that influences the part temperature and the thermal history. To investigate this influence, cylinders with a diameter of 10 mm and a height of 40 mm are constructed with a constant layer time of t_{s_min} = 16.68 s. The thermal history of the part is also influenced by the part temperature. Up to a part height of 30 mm, the basic parameter set is used. The surface energy E_F can be adjusted via the parameters laser power, scanning speed or hatch distance. However, only an adjustment of the laser power is carried out within the scope of this work. From a defined part height, a sample with a power of 180, 160, 140, and 120 W is built. To create a wider data basis, which also takes into account different geometries, further tests are carried out. These include different cross-section shapes (triangles, cuboids, cylinders) with different cross-section sizes (20–400 mm²), different layer times (16.68–155 s) and further variations of the laser power (120–195 W). The training data have a total scope of 1607 data sets. The temperature measurement is analogous to the previous test. The test is repeated four times and the mean value of the temperature curves is calculated. To investigate the influence of the reduced laser power on the part properties, the upper part of the samples is cut off and a density measurement is carried out. The density

measurement is carried out analogously to the procedure of Spierings et al. according to the Archimedean measuring principle [13]. For this purpose, the weight of the samples (m_s) is first determined with a precision balance of the type ABT 220-4M (KERN & SOHN GmbH, Frommern, Germany) with a measuring accuracy of ± 0.1 mg. Subsequently, the samples are immersed with a special sample carrier in a 5% soap solution and the weight is determined again (m_l). Before this, the temperature-dependent density of the liquid is determined using a potassium-plated test body. To determine the influence of the part temperature on the mechanical properties of the parts, tensile specimens of type A according to DIN 50125 [14] with a specimen diameter of 5 mm and a measuring length of 25 mm are produced from the manufactured cylinders. No heat treatment and stress relieving is done. The tensile test is carried out with a tensile compression test system of type Z100 (ZwickRoell GmbH & Co. KG, Germany, Ulm) with a maximum test load of 100 kN. The specimen elongation is measured optically with a video extensiometer that achieves class 1 accuracy according to DIN EN ISO 9513 [15]. The tensile test is carried out path-controlled at a speed of 0.1 mm/s.

3. Development of a module for predicting the thermal history

To be able to make the best possible prediction of the part temperature history, all parameters that influence temperature development must be known and made available to the neural network as input variables. There are boundary conditions that are dependent on the part geometry, boundary conditions that are dependent on the material and on the used process parameter set, as well as global- and layer-dependent boundary conditions. Based on the state-of-the-art, the boundary conditions listed in Table 1, which serve as input parameters for the neural network, are identified. Boundary conditions that do not change throughout the entire process, for example, the physical material properties or machine-specific properties such as the size of the installation space, are not included because they have the same influence on the result in each layer. The energy input into the part is also reduced to the laser power, since the other energy parameters scanning speed, hatch distance and layer thickness are fixed. The parameters t_s, b_{th}, A_s, V_s, V_g, A_{ps} and A_{pg} are calculated by the known variables. The laser power is variable. The two factors for layer time change k_{ts_n} and cross-section change k_{As_n} are calculated using equations 1 and 2. These serve to consider strong changes in the cross-sectional area and thus also in the stratum time.

$$k_{ts\_n} = \frac{t_{s\_n} \cdot 5}{\sum_{k=n-5}^{k=n-1} t_{s\_k}} \quad \text{(Eq. 1)}$$

$$k_{As\_n} = \frac{A_{s\_n} \cdot 5}{\sum_{k=n-5}^{k=n-1} A_{s\_k}} \quad \text{(Eq. 2)}$$

The experimental data from the previous experiments are used as the basis for setting up the neural network. The goal of the network is to predict the part temperature layer by layer before the melting process. The data are thus also provided layer by layer. For each layer, there are ten input parameters and one output parameter in the form of the temperature averaged over the cross-section. The experimental test series with different layer times, geometries and laser powers serve as a basis.

Table 1: Input parameters for the neural network

Type	Name	Sy.	Unit
Layer based	Layer time	t_s	s
	Deviation in layer time	k_{ts}	-
	Part height	b_{th}	mm
Energy input	Laser power	P_L	W
Geomtric	Cross-sectional area	A_s	mm²
	Deviation in cross-sectional area	k_{As}	-
	Layer volume	V_s	mm³
	Accumulated volume	V_g	mm³
	Area enclosed by powder	A_{ps}	mm²
	Accumulated area enclosed by powder	A_{pg}	mm²

The Deep Learning Toolbox from Matlab (version 2017b) is used to create the neural network. The command *fitnet* creates a two-layer feedforward network with sigmoid neurons in the hidden layer and linear neurons in the output layer. The number of neurons in the hidden layer has a large influence on the quality of the prediction. If the number is too low or too high, the network may be under- or over-determined. In case of under-determination, the network cannot map all phenomena that are present in the input data. In the case of over-determination, too little information is available to train all neurons, the training time is increased and the memory requirement of the network increases. According to Heaton, the number of neurons should be between the number of input parameters and the number of output parameters [16]. To find a suitable number of hidden neurons, the neural network is trained in a series of experiments with varying numbers of 2–10 neurons. Of the data sets, 70% are used for training, 15% for validation and 15% for testing the quality of the network. Since the selection of data sets is random, training is performed 15 times with each number of neurons to determine the dispersion of results. The training algorithm used is the Levenberg-Marquardt method [17]. To assess the quality of the network, the mean square deviation and the coefficient of determination are used. The result of the test series is shown in Figure 3. The mean square deviation decreases and thus the coefficient of determination also increases with an increasing number of hidden neurons. From a number of seven neurons upwards, no significant improvement can be observed in the present training data set. For further experiments, a network with seven neurons in the hidden layer is used.

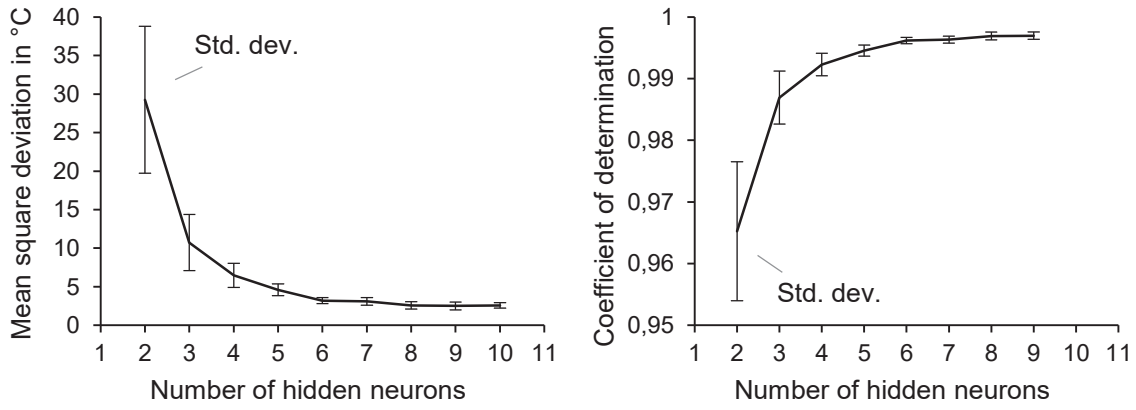

Figure 3: Influence of the number of neurons on the quality of the prediction

Based on the layer-wise statistics and the process boundary conditions, an input matrix is generated in the first step, in which the parameters shown in Table 1 are stored for each layer. The layer time is calculated according to equation 2. If a value for the minimum layer time is stored and the calculated layer time is less than the minimum layer time, this value is used instead. With the help of the input matrix and the already trained neural network, a prediction of the averaged temperature over the entire part surface can now be calculated. The curves of the measurement results and the prediction of the neural network have a high agreement, which shows that in this case, the network can be used to predict the temperature. The prediction module is also tested on a demonstrator construction job. For this purpose, seven randomly generated parts with heights of 37-73 mm and varying cross-sections are built in one job (Figure 4). Three of the seven parts also have an internal cavity.

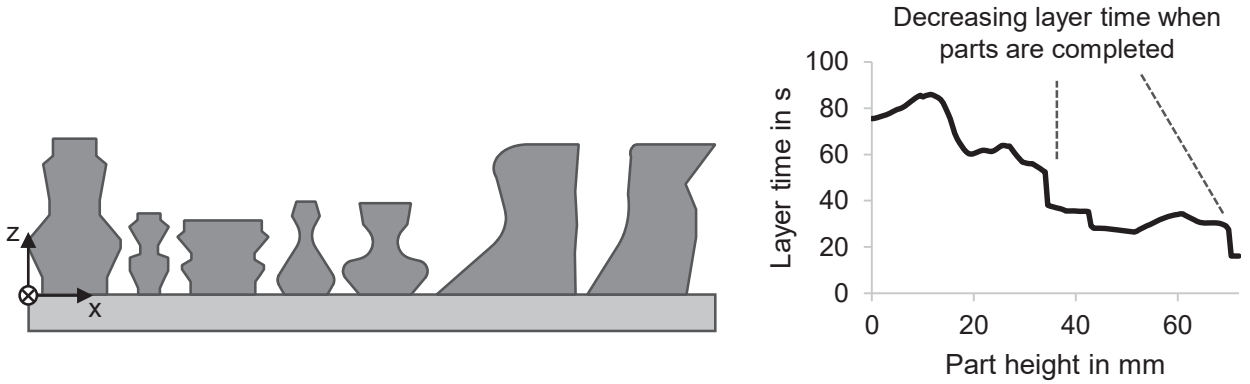

Figure 4: Complex Geometries (left) and relating layer times of the building process (right)

At a part height of 14 mm, the temperature in the part rises only slightly due to the long layer times. The increase in the cross-sectional area in combination with the reduction in the layer time (Figure 4) leads to a temperature rise to 120 °C at a height of 23.5 mm (Figure 5). The reduction of the cross-sectional area then causes a drop in temperature at a constant layer time. The sharp drop in the layer time at 34-mm height causes a sudden short-term rise in temperature. The smallest cross-sectional area is at a part height of 51 mm. After this height, the largest temperature increase to 167 °C can be observed. In addition to the short layer time, this can be explained by the reduced thermal conductivity of the small cross-section. With a further reduction of the cross-sectional area, the temperature drops again and then rises again to 166 °C at the very short layer time of 16 s.

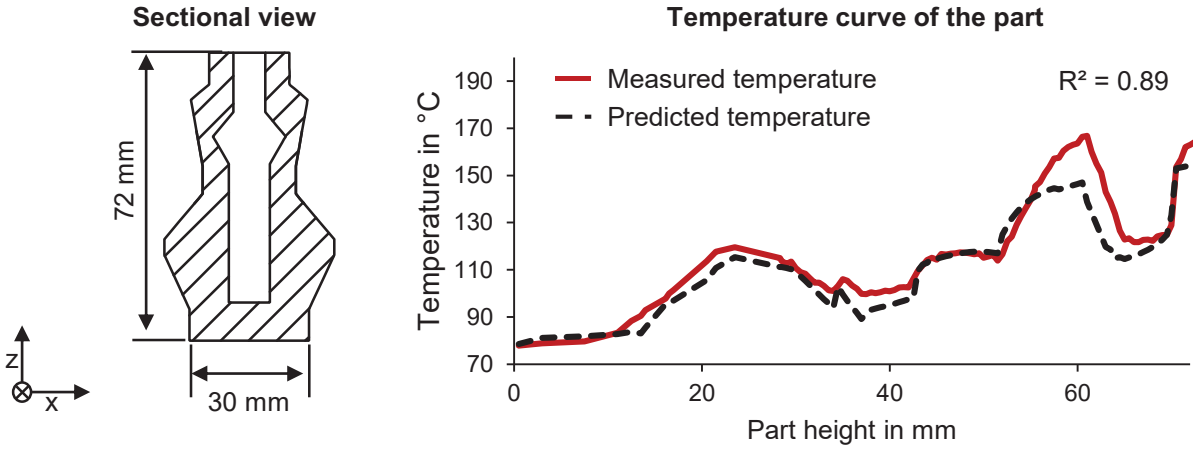

Figure 5: Comparison of measured and predicted temperature (right) for a complex geometry (left)

4. Controlling the thermal history

There are two options to control the part temperature. On the one hand, the temperature can be adjusted by adjusting the layer time or the energy input into the part. As the temperature control by adjusting the layer time leads to additional waiting time, this option is not reasonable for industrial use. To control the thermal history via the energy input, the neural network is used. The neural network is designed only to predict a part temperature together with the given laser powers and the other boundary conditions. For the inverted case, a new network would have to be trained to predict the required laser power at given temperatures. The experiments in section 5.4 have shown, however, that the laser power cannot be adjusted arbitrarily, as this would lead to the formation of porosity when the laser power is too low. Therefore, an approach is used that determines the range in which the power can be adjusted and in which the existing neural network can be used. Shortly after the reduction of the laser power, a drop of the part temperature depending on the laser power can be detected. At the same time, however, an increase in temperature, even with the reduced laser power, can be seen in the further course. No significant reduction in part density can be seen with the 180- and 160-W power ratings. At a power of 140 W, a small drop in density can be measured and at a power of 120 W, a significant drop of 0.5% can be observed (Table 2). Therefore, a laser power of 140 W should not be undercut to prevent the part of porosity. The layer time is constantly set to 25s, as measurement data are already available for this.

Table 2: Results of density measurement for reduced laser power

Laser Power [W]	Density [g/cm³]	Std. Dev. [g/cm³]	relative Density*
Basic parameter set	7.9911	0.0009	100.00 %
180 W	7.9921	0.0013	100.01 %
160 W	7.9908	0.0016	100.00 %
140 W	7.9876	0.0023	99.96 %
120 W	7.9508	0.0030	99.50 %

* Reference: 7,9911 g/cm³ (basic parameter set)

The next step is to determine which maximum or minimum temperatures should not be exceeded or fallen below. These values must be determined individually for each material building and testing tensile specimen with specific layer times and therefore specific temperatures. Furthermore, it must be determined in which case the laser power may be adjusted upwards or downwards to influence the part temperature. Via the neural network, the layers are now identified at which the intended temperature window is left. For each of these layers, an input matrix for the neural network is generated, in which the laser power is varied between the minimum and maximum permissible values. The output vector is then compared with the target temperature and the laser power with the smallest deviation is stored for the respective layer. The output matrix in which the laser power for all voxels is adjusted layer by layer is then generated. To validate the module, cylindrical specimens for tensile tests with a diameter of 10 mm and a height of 75 mm are fabricated in which the part temperature is to be specifically controlled. The mechanical properties of the material used in this work can be reduced at elevated part temperatures. Therefore, a process control is to be determined at which a part temperature of 110°C is not exceeded. Measurement and prediction show that from a part height of 27 mm, the target temperature of 110°C is exceeded. With the help of the process module, a construction job is now created in which

the laser power is adjusted from this height to prevent the temperature rise. This initially drops sharply until it remains constant at the minimum permissible laser power of 140 W, with a part height of 68.1 mm. The averaged temperature curve of all samples is shown in Figure 6 (right). The curve is identical to the reference test up to a part height of 26 mm. The target temperature of 110°C is reached in the range between 27 and 47 mm. From a part height of 47 mm, a slight increase in temperature can be seen, which is stronger than that from a part height of 68 mm. The final temperature is 114.79°C.

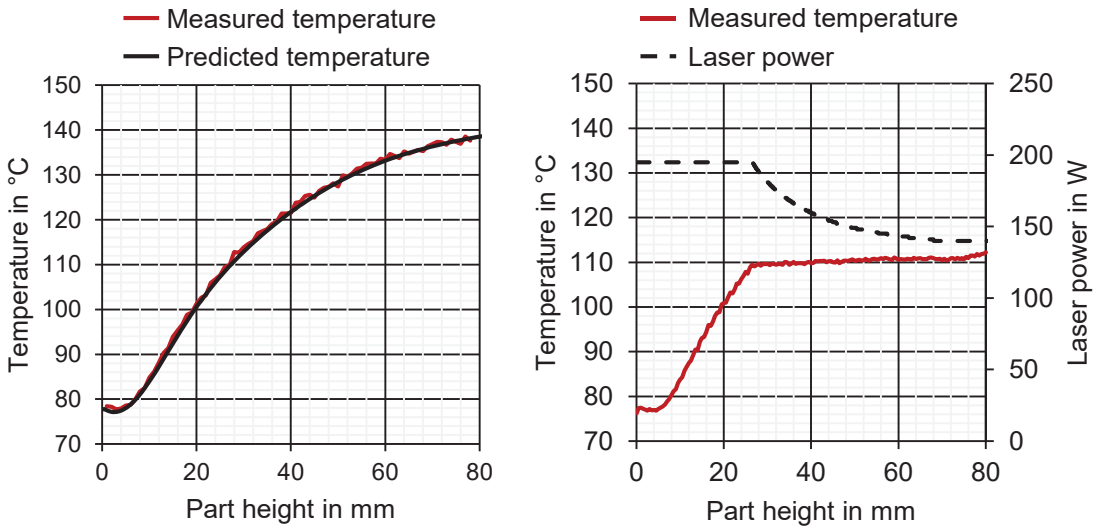

Figure 6: Temperature curve for an unadjusted process (left) an adjusted laser power (right)

5. Mechanical Characterization

To evaluate the influence of the part history, the mechanical characteristics are taken into account. An average increase in tensile strength of 19.84 MPa and an average increase in yield strength of 24.16 MPa can be observed in the specimens with adapted temperature control. The elongation at break, on the other hand, decreases on average by 5.15%. On the right side of Figure 7 the distribution of the laser power within the tensile specimen is shown. Failure occurred in the marked fracture zone in all specimens of the test. This is in the lower area of the test zone, where the power is higher than in the upper area.

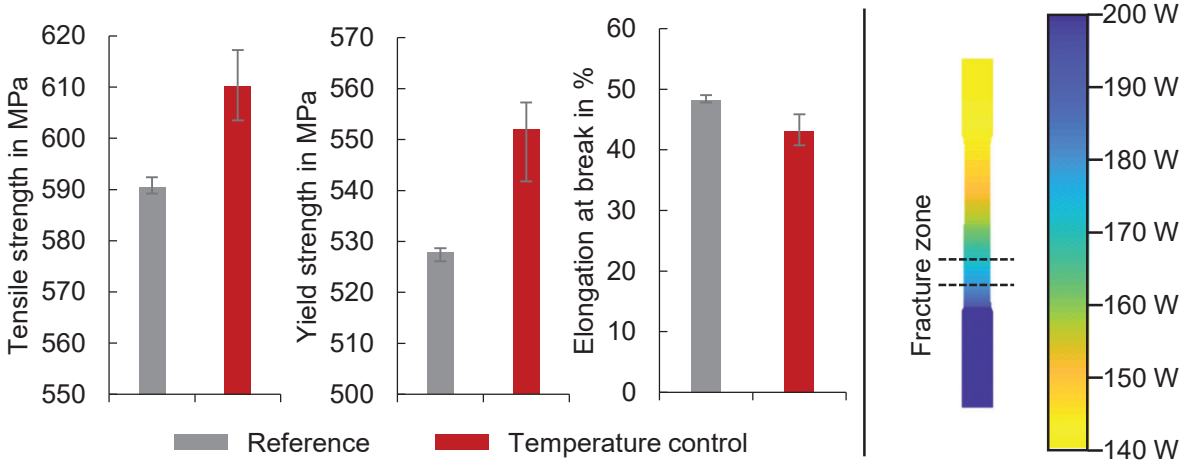

Figure 7: Results of the tensile tests

6. Discussion

In fact, there are two options to adjust the thermal history. Since the process cannot be accelerated due to the given part geometry in order to reduce the layer times, only a reduction of the temperature can be achieved by increasing the minimum layer time over the layer time. However, this affects all parts on the building platform and can therefore lead to unwanted temperature reductions in other parts. In the sense of a part-specific process control, this work therefore carries out a temperature control by adjusting the laser power. Since the adaptation, however, results in a change of the area energy, the mechanical properties of the part may change. The prediction of the thermal history via the neural network with a coefficient of determination of R^2=0.89 shows a high qualitative conformity with the real temperature curve. In some areas, however, the actual temperature of the part is underestimated. This can be caused either by a too small amount of training data or by the factors for cross-sectional and layer time changes. The neural network mainly uses the information of the underlying layer for temperature prediction. The change factors also provide information about the course of the last five layers. However, the temperature curve shown in Figure 5 indicates that the knowledge of only five layers is not sufficient to describe the strong temperature rise at the part height of 60 mm.

By adjusting the laser power, the mechanical properties of the material change towards a more brittle material behavior. The material behaviour in the test area is therefore graded, with failure always occurring at the weakest point. A similar behaviour can also be observed with a combination of different parameter sets within a tensile test [18].

7. Summary and outlook

In this work, a process analysis module is developed for predicting and controlling averaged part layer temperatures. The basis is a neural network, which is trained with a comparatively small data set. The reliability of the temperature prediction for simple part geometries is very good and represents the actual temperature curve. The control of the part temperature can be done via the input energy in the form of a reduction or increase of the laser power. Within the given boundary conditions, the part temperature can be controlled specifically with the aid of the neural network. The adjustment of the laser power, however, also has an influence on the mechanical properties of the material. For the selected material, however, this is to be evaluated as positive. In practice, it must be determined for each material at which temperatures critical effects such as precipitation or undesired phase formation occur. If the material reacts negatively to a change in the laser power, the layer time must be adjusted instead. This can be done either by adding specific waiting times or by optimizing the arrangement of the parts on the construction platform. The neural network can be used to support such an optimization. Metallographic analysis can further contribute to the understanding of the changed mechanical properties.

Acknowledgments

This research and development project is funded by the German Federal Ministry of Education and Research (BMBF) within the “Innovations for Tomorrow’s Production, Services, and Work” Program (funding number 02P15B030 – 02P15B036) and implemented by the Project Management Agency Karlsruhe (PTKA). The author is responsible for the content of this publication.

References

[1] Deutsches Institut für Normung e. V. Additive Fertigung - Grundlagen - Terminologie(52900). Berlin: Beuth Verlag GmbH; 2018. [May 24, 2019].

[2] Gu DD, Meiners W, Wissenbach K, Poprawe R. Laser additive manufacturing of metallic components: materials, processes and mechanisms. International Materials Reviews 2012;57(3):133–64.

[3] Hirsch M, Patel R, Li W, Guan G, Leach RK, Sharples SD et al. Assessing the capability of in-situ nondestructive analysis during layer based additive manufacture. Additive Manufacturing 2017;13:135–42.

[4] Neef A, Seyda V, Herzog D, Emmelmann C, Schönleber M, Kogel-Hollacher M. Low Coherence Interferometry in Selective Laser Melting. Physics Procedia 2014;56:82–9.

[5] Kolb T, Müller L, Tremel J, Schmidt M. Melt pool monitoring for laser beam melting of metals: inline-evaluation and remelting of surfaces. Procedia CIRP 2018;74:111–5.

[6] Grasso M, Colosimo BM. Process defects and in situ monitoring methods in metal powder bed fusion: a review. Meas. Sci. Technol. 2017;28(4):44005.

[7] Chivel Y. Optical In-Process Temperature Monitoring of Selective Laser Melting. Physics Procedia 2013;41:904–10.

[8] Zur Jacobsmühlen J, Kleszczynski S, Witt G, Merhof D (eds.). Elevated Region Area Measurement for Quantitative Analysis of Laser Beam Melting Process Stability; 2015.

[9] Coeck S, Bisht M, Plas J, Verbist F. Prediction of lack of fusion porosity in selective laser melting based on melt pool monitoring data. Additive Manufacturing 2019;25:347–56.

[10] Hooper PA. Melt pool temperature and cooling rates in laser powder bed fusion. Additive Manufacturing 2018;22:548–59.

[11] Krauss H, Zeugner T, Zaeh MF. Layerwise Monitoring of the Selective Laser Melting Process by Thermography. Physics Procedia 2014;56:64–71.

[12] Verein deutscher Ingenieure e.V. Technische Temperaturmessung - Strahlungsthermometrie - Praktische Anwendung von Strahlungsthermometern(3511 Blatt 4.5); 2015.

[13] Spierings AB, Schneider M, Eggenberger R. Comparison of density measurement techniques for additive manufactured metallic parts. Rapid Prototyping Journal 2011;17(5):380–6.

[14] Deutsches Institut für Normung e. V. Prüfung metallischer Werkstoffe - Zugproben(50125). Berlin: Beuth Verlag GmbH; 2016.

[15] Deutsches Institut für Normung e. V. Metallische Werkstoffe - Kalibrierung von Längenänderungsmesseinrichtungen für die Prüfung mit einachsiger Beanspruchung(9513). Berlin: Beuth Verlag GmbH; 2013.

[16] Heaton J. Introduction to neural networks with Java. 2nd ed. St. Louis, Mo.: Heaton Research; 2008.

[17] Hagan MT, Menhaj MB. Training feedforward networks with the Marquardt algorithm. IEEE Trans Neural Netw 1994;5(6):989–93.

[18] Kniepkamp M, Harbig J, Seyfert C, Abele E (eds.). Towards High Build Rates: Combining Different Layer Thicknesses within one Part in Selective Laser Melting; 2018.